



Experimental study on the lateral-torsional buckling strength of trapezoidally corrugated web girders

Bence Jáger¹, Balázs Kövesdi², László Dunai³

Abstract

Current standards and specifications do not provide design methods to determine the lateral-torsional buckling (LTB) strength of girders with trapezoidally corrugated web. In the international literature there is only a limited number of previous investigations available focusing on the LTB strength of corrugated web girders. Based on numerical calculations analytical solutions have been derived in the past, however, there is a lack of experimental test results to prove or improve these design proposals. Therefore, the authors performed an extensive experimental research program in the Structural Laboratory of the Budapest University of Technology and Economics including eleven large-scale test specimens. All the test girders have different flange sizes, beside, having the same corrugation profile. The test specimens are loaded by pure in-plane bending having simply supported boundary conditions. The buckling length of the specimens is 6000 mm with limited warping and rotational restraint at the supports. During the tests the longitudinal stresses are captured at characteristic points and the displacements in vertical and lateral directions are measured as well as the rotation of the middle cross-section. The measured strength of the test specimens is compared to the analytical proposals regarding corrugated web girders and the differences are evaluated. Based on the experimental results an improved design method is proposed for the determination of the lateral-torsional buckling strength of trapezoidally corrugated web girders.

Keywords: corrugated web; trapezoidal corrugation; lateral-torsional buckling; bending moment resistance.

1. Introduction

Corrugated web girders are increasingly used in the structural engineering praxis due to their numerous favorable properties. The local and global member stability has a greater importance in the design of these girders. In the international literature the effect of local stability on cross-sectional resistances, namely the (i) bending moment resistance, (ii) shear buckling resistance and (iii) resistance against transverse force have been extensively studied by researchers in the past and there are accurate design models available for the determination of these resistances.

¹ PhD Student, Budapest University of Technology and Economics, <jager.bence@epito.bme.hu>

² Associate Professor, Budapest University of Technology and Economics, <kovesdi.balazs@epito.bme.hu>

³ Professor, Budapest University of Technology and Economics, <dunai.laszlo@epito.bme.hu>

The global member stability, namely the lateral-torsional buckling strength of corrugated web girders was first investigated by Lindner (1990). Since then a few researchers studied the elastic critical moment and ultimate strength of corrugated web girders. There is agreement between researchers that the elastic critical moment of corrugated web girders is greater than those of with flat webs. The increment has been, however, considered in different ways by attributing to different cross-sectional properties. Furthermore, the ultimate lateral-torsional buckling strength has been investigated mainly by nonlinear FE analysis in the past; the number of available test results is limited. Therefore, the current paper focuses on the experimental study of 11 large-scale test specimens investigating the lateral-torsional buckling resistance of corrugated web girders. Based on the test results, the previous design proposals are compared, evaluated and a design model is proposed for the lateral-torsional buckling strength of trapezoidally corrugated web girders. The applied notations in the paper are given in Fig. 1.

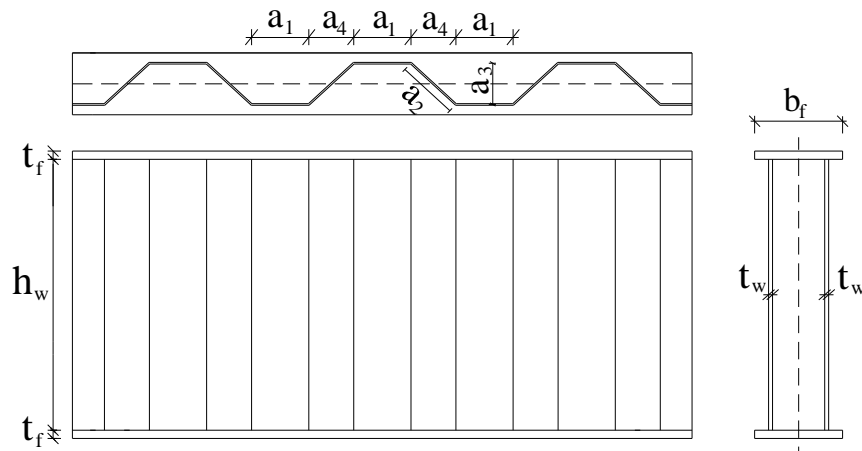


Figure 1: Applied notations

2. Literature review

The lateral-torsional buckling strength of corrugated web girders was first investigated by Lindner (1990). Since then several researchers investigated the elastic critical moment by FE buckling analysis and theoretical studies. The ultimate strength and applicable buckling curves were investigated by nonlinear FE analysis and experimental studies. In addition, researchers investigated different boundary and loading conditions and their influence on the elastic critical moment. This section collects the previous studies dealing with the lateral-torsional buckling strength of trapezoidally corrugated web girders.

2.1 Investigations on the elastic critical moment

The elastic critical moment of a conventional flat web girder subjected to uniform bending moment can be calculated by Eq. 1 according to EN1993-1-1 and Timoshenko and Gere (1961).

$$M_{cr} = \frac{\pi^2 \cdot EI_z}{(k \cdot L)^2} \sqrt{\left(\frac{k}{k_w}\right)^2 \cdot \frac{I_w}{I_z} + \frac{(k \cdot L)^2 \cdot GI_t}{\pi^2 \cdot EI_z}} \quad (1)$$

In the above equation L is the span of the girder, E is the elastic modulus, G is the shear modulus, I_z is the moment of inertia about the minor axis, I_t is the torsional constant, I_w is the

warping constant, k is the effective length factor about the weak axis rotation and k_w is the effective length factor with respect to warping.

In the past several researchers found that the elastic critical moment of the trapezoidally corrugated web girders and their ultimate strength is greater than that of girders with conventional flat webs (Sayed-Ahmed 2005, Moon et al. 2009, Nguyen et al. 2010, Zhang et al. 2011, Larsson and Persson 2013, Ilanovsky 2015). The increase in the elastic critical moment has been, however, attributed to different sectional properties by different authors. Most of the researchers agree that the web contribution should be ignored in the moment of inertias about the strong and weak axes, but there are contradictions in the consideration of the increased elastic critical moment. Firstly, Lindner (1990) suggested an additional term with a correction factor c_w in the warping constant given by Eqs. 2-4 for double symmetric sections in order to consider the greater performance ($c_1=8$, $c_2=25$); where $I_{w,flat}$ is the warping constant of flat web girder.

$$I_w = I_{w,flat} + c_w \frac{L^2}{E\pi^2} \quad (2)$$

$$c_w = \frac{a_3^2 \cdot (h_w + t_f)^2}{c_1 \cdot u_x \cdot (a_1 + a_4)} \quad (3)$$

$$u_x = \frac{(h_w + t_f)}{2 \cdot G \cdot a_1 \cdot t_w} + \frac{(h_w + t_f)^2 \cdot (a_1 + a_4)^3}{c_2 \cdot a_1^2 \cdot E \cdot b_f \cdot t_f^3} \quad (4)$$

Moon et al. (2009), Nguyen et al. (2010), Zhang et al. (2011) and Ibrahim (2014) also proposed that the greater performance should be taken into account in the warping constant and new additional terms were developed. Larsson and Persson (2013) performed a notable FE study and found that the proposal of Lindner (1990) gives the best approximation to the numerical results. However, this additional term depends on the girder length being not possible for a sectional constant. Therefore, they substituted the Lindner's proposal into Eq. 1 in order to rearrange the additional term to the torsional constant according to Eq. 5.

$$I_t = I_{t,flat} + \frac{c_w}{G} \quad (5)$$

The appropriateness of Eq. 5 was confirmed by Lopes et al. (2017) and they proposed a slightly modified correction factor c_w for trapezoidally and sinusoidally corrugated web girders ($c_1=22$, $c_2=300$ in Eqs. 3-4) based on FE analysis. In addition, Guo and Papangelis (2018) comparatively studied the torsional behavior of trapezoidally corrugated and flat web girders subjected to uniform and non-uniform torsion. Their FE analysis showed that the torsional constant of corrugated web girders is significantly greater than those of with flat web, however, there is just a minor difference between the warping constants.

Other proposals were also applied for the consideration of the greater performance by using equivalent web thickness (Sayed-Ahmed 2005), reduced shear modulus (Moon et al. 2009,

Nguyen et al. 2010, Ibrahim 2014, Kazemi 2010) or using a simple multiplication factor on the elastic critical moment of flat web girders (Ilanovsky 2015).

In addition, some research activities were focusing on different loading and boundary conditions as well. Nguyen et al. numerically studied different end restraint conditions of simply supported girders considering (i) the concentrated load height effect for three-point-bending loading condition (2011a), (ii) the tapered configuration (2011b), and (iii) the different moment gradients along the girder length (2012). The effect of linear moment gradient was also studied by Moon et al. (2013) and Lopes et al. (2017). Based on the FE results new moment modification factors are proposed on the elastic critical moment for corrugated web girders.

2.2 Investigations on the lateral-torsional buckling strength

The ultimate lateral-torsional buckling strength of corrugated web girders have been studied through only a few number of experimental tests and some nonlinear FE analysis by different researchers. The lateral-torsional buckling strength was experimentally investigated under three-point-bending by Kubo and Watanabe (2007) on nine trapezoidally corrugated web girders and Hannebauer (2008) and Pimenta et al. (2015) on three and four sinusoidally corrugated web girders, respectively. In addition, Zhang et al. (2017) tested four sinusoidally corrugated web girders using a cantilever arrangement with concentrated load introduction at the end of the cantilever.

According to EN1993-1-1 the reduction factor (χ_{LT}) for the lateral-torsional buckling strength for rolled sections or equivalent welded sections with flat web may be calculated by Eqs. 6-8, where α_{LT} is the imperfection factor (for different buckling curves: $a - 0.21$, $b - 0.34$, $c - 0.49$, $d - 0.76$), $\bar{\lambda}_{LT}$ is the relative slenderness, β is the multiplication factor and $\bar{\lambda}_{LT,0}$ is the relative slenderness limit. The standard suggests to use buckling curve d if the depth-to-width ratio of the section is greater than 2; otherwise the buckling curve c shall be used. In Eq. 8 M_y is the cross-sectional bending moment resistance considering the local flange buckling as given by Eq. 9.

$$\chi_{LT} = \frac{1}{\Phi_{LT} + \sqrt{\Phi_{LT}^2 - \beta \bar{\lambda}_{LT}^2}} \text{ but } \chi_{LT} \leq \min\left(1.0; \frac{1}{\bar{\lambda}_{LT}^2}\right) \quad (6)$$

$$\Phi_{LT} = \frac{1 + \alpha_{LT} \cdot (\bar{\lambda}_{LT} - \bar{\lambda}_{LT,0}) + \beta \bar{\lambda}_{LT}^2}{2} \quad (7)$$

$$\bar{\lambda}_{LT} = \sqrt{\frac{M_y}{M_{cr}}} \quad (8)$$

Nonlinear FE analyses have been conducted by Moon et al. (2009, 2013) and it is concluded that the use of the buckling curve b ($\beta=1.0$ and $\bar{\lambda}_{LT,0}=0.2$) of EN1993-1-1 results in conservative solutions for trapezoidally corrugated web girders. Ibrahim (2014) performed nonlinear FE analysis on trapezoidally corrugated web girders with unequal flanges and found that the lateral-torsional buckling curve d of EN1993-1-1 is applicable using $\beta=0.75$ and $\bar{\lambda}_{LT,0}=0.4$. Elkawas et

al. (2018) numerically studied high-strength steel trapezoidally corrugated web girders and found that the lateral-torsional buckling curve a could be applicable using $\bar{\lambda}_{LT,0}=0.4$.

2.3 Conclusions on the literature review

Previous research results showed that the elastic critical moment of corrugated web girders is greater than those of with flat web and the increase is mostly attributed to the greater torsional constant due to the alternating eccentricity of the web. Nonlinear FE analyses are also performed by some researchers and found that the ultimate strength may be determined by the lateral-torsional buckling curve of the EN1993-1-1 using $\beta =0.75$ and $\bar{\lambda}_{LT,0}=0.4$. However, the available test results are very limited to prove the applicability of any of the previous proposals.

3. Experimental research program

3.1 Test specimens

Experimental research program is performed in 2018 at the Budapest University of Technology and Economics, Department of Structural Engineering in Hungary. In the frame of the research program 11 large-scale test specimens are examined by four-point-bending condition. Six different girder geometries having different flange sizes and the same trapezoidal corrugation profile are investigated. Further 5 specimens are used for test duplications investigating the accuracy of the results. The measured geometrical and material properties of the tested girders and the notations are summarized in Figs. 2-3 and in Table 1. For all the specimens the widths of the parallel and inclined web folds are equal ($a_1=a_2=98$ mm) as mainly used in bridges with a corrugation angle of 45° .

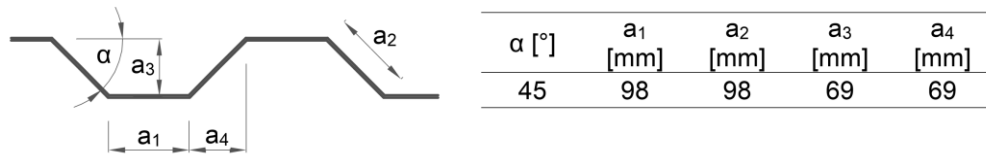


Figure 2: Applied trapezoidal corrugation profile

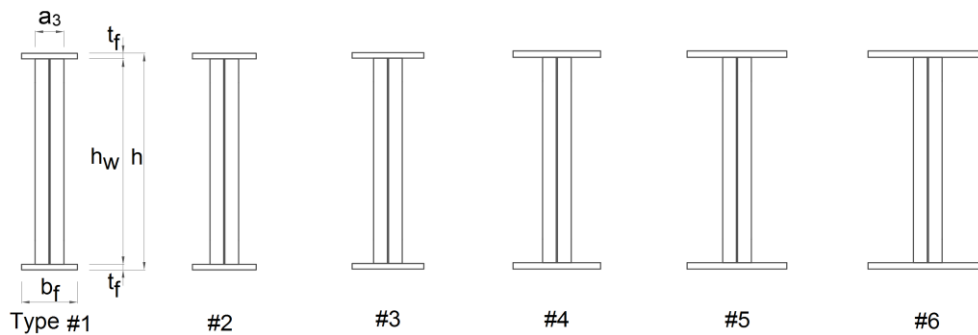


Figure 3: Cross-sectional layout of specimen's geometry

Figure 3 presents the scaled drawings of the six specimen types having different flange sizes; the numbering of the girders is set accordingly in the order of increasing flange sizes. The nominal flange thickness (t_f) of specimen type #1, #2, and #3 is 14 mm, while it is 16 mm for specimen type #4, #5, and #6 tabulated in the second column of Table 1. The nominal flange widths (b_f) are 140, 160, 180, 220, 250, and 300 mm, respectively. The thickness of the web (t_w) is 6 mm for

all specimens with a nominal web depth (h_w) of 520 mm. At the load introduction and support locations vertical stiffeners are placed with a nominal thickness (t_s) of 10 to 16 mm. The specimens are designed to cover a wide range of different LTB slenderness ratios to characterize the lateral-torsional buckling behavior of corrugated web girders. The steel material has a prescribed steel grade of S355 for flanges and S235 for the web with a nominal yield strength of 355 MPa and 235 MPa, respectively. The material properties are evaluated by coupon tests according to ISO 6892-1. Results can be found in the last columns of Table 1 regarding the flange yield (f_{yf}) and ultimate strength (f_{uf}) and web yield (f_{yw}) and ultimate strength (f_{uw}), respectively.

Table 1: Measured geometrical and material properties of the test specimens

Specimen	t_f (mm)	b_f (mm)	t_w (mm)	h (mm)	h_w (mm)	t_s (mm)	f_{yf} (MPa)	f_{uf} (MPa)	f_{yw} (MPa)	f_{uw} (MPa)
1/1	13.8	139	6	547.0	519.3	10	357	528	289	379
1/2	14.1	140	6	545.5	517.3	10	357	528	289	379
2/1	14.0	158	6	548.5	520.6	10	357	528	289	379
2/2	14.0	162	6	546.5	518.4	10	357	528	289	379
3/1	14.0	181	6	546.5	518.5	14	357	528	289	379
3/1	14.0	179	6	548.0	520.0	14	357	528	289	379
4/1	16.7	219	6	553.0	519.6	14	379	534	289	379
5/1	16.5	250	6	552.0	519.0	14	379	534	289	379
5/2	16.6	250	6	550.0	516.8	14	379	534	289	379
6/1	15.9	300	6	551.0	519.1	16	372	520	289	379
6/2	16.1	300	6	550.0	517.9	16	372	520	289	379

3.2 Test setup

The applied test arrangement is presented in Fig. 4. The general purpose of the test layout is to apply large clear span (6000 mm), ensuring large buckling length. The total length of the tested girders is 8.2 m. The specimens are vertically supported at the cross-sections 1100 mm from both ends. The concentrated vertical forces are introduced at the end cross-sections (100 mm from both ends) creating a four-point-bending loading condition with lever arms of 1000 mm. The load is produced by two hydraulic jacks with maximum loading capacities of 1000 kN. The concentrated transverse force is introduced through rigid steel load transfer elements placed on the upper flange. The girders are laterally supported at the vertical supports and load introduction places in order to restrain the out-of-plane rotation, thus to anchor the transverse bending moment. In addition, the specimens are strengthened by vertical stiffeners at the locations of vertical supports and load introduction places in order to avoid local failure. By this setup the twist and warping are restrained, so thus the torsional moment is anchored; bimoment can develop. Furthermore, the two 1000 mm long cantilevers are strengthened by braces as shown in Fig. 5 to improve the shear strength and avoid premature shear buckling failure of the test girders. The specimens are equipped by linear variable displacement transducers (LVDTs) and strain gauges which are shown in Figs. 4-6 and tabulated in Table 2. During the tests the 3 DOFs movement of the middle cross-section is captured, namely the (i) deflection, (ii) lateral displacement and (iii) rigid body rotation by using a rigid frame equipped with four LVDTs denoted by T1-4. These LVDTs are attached in one point to the specimen's bottom (T1-2) and

top (T3-4) flanges with diagonal wiring via steel rollers. The diagonal wires create two scalene triangles with changing edges during the tests. Since four LVDTs are attached the measurement system is overdetermined for the derivation of the 3 DOFs movement giving a control option for the evaluation. Beside, an additional vertical LVDT is used denoted by T5 in order to control T1-4 in elastic state.

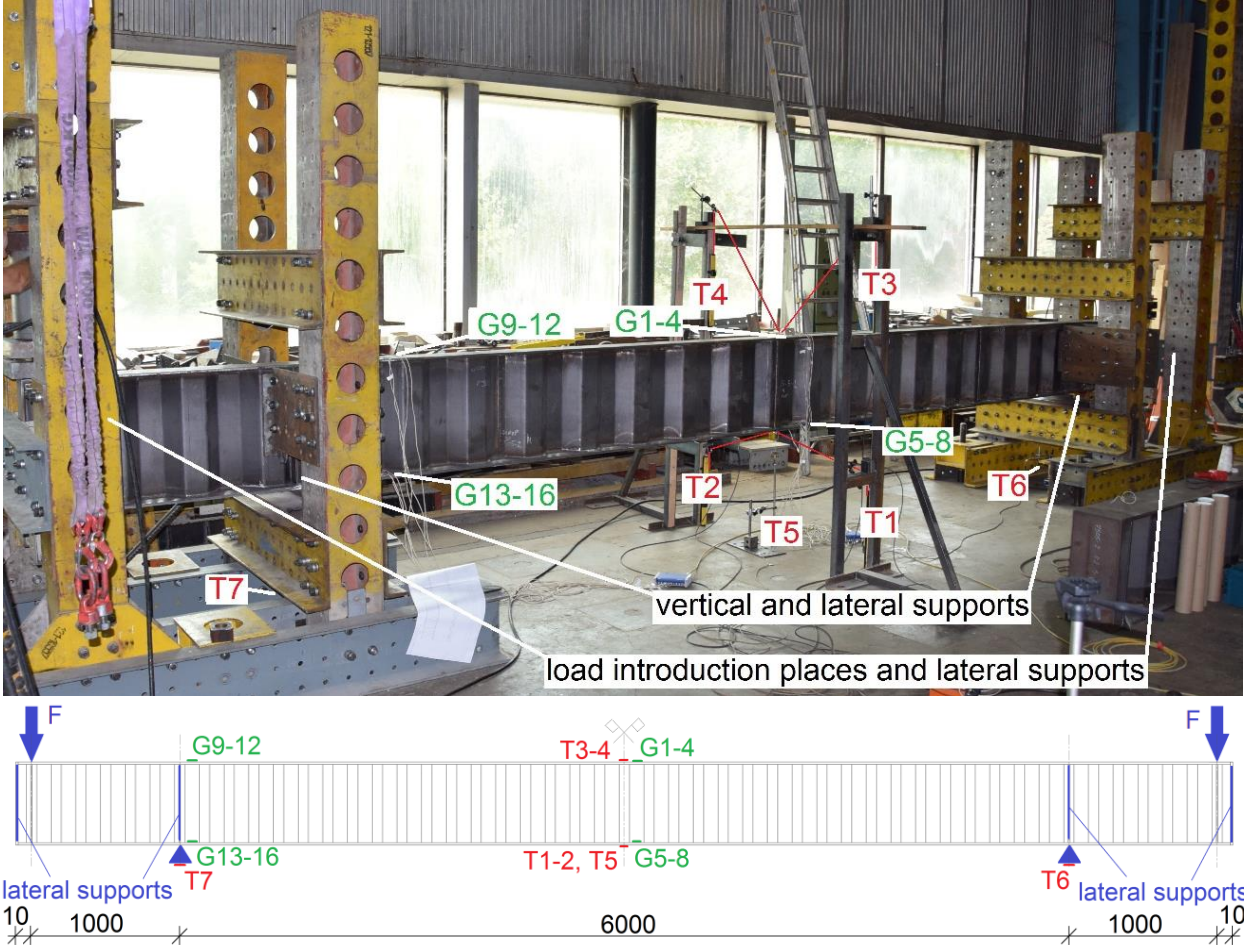


Figure 4: Test setup and location of measuring devices

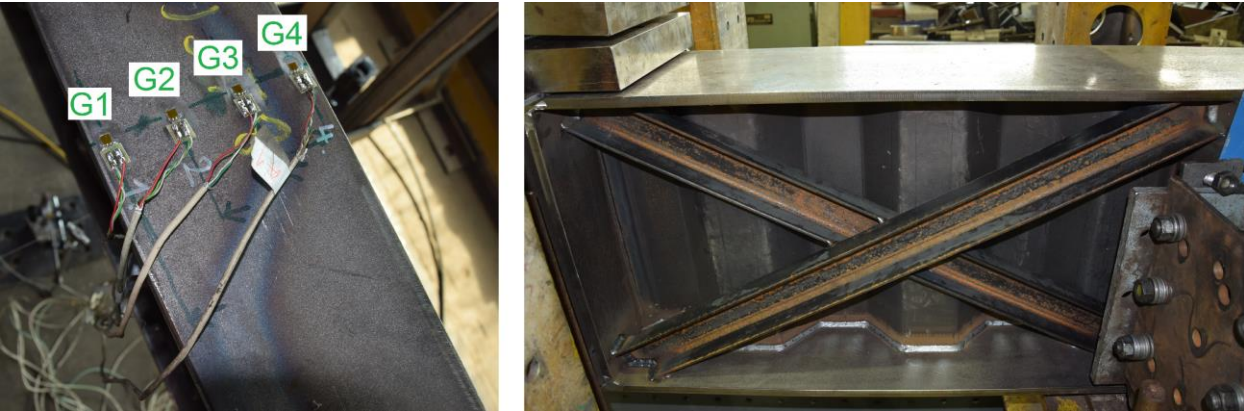


Figure 5: Strain gauge distribution on the top flange and shear strengthening of cantilever parts

The strains are also captured at characteristic points of the specimens by strain gauges denoted by G1-16 in Figs. 4-5 and Table 2. The strain gauges are attached to the upper surfaces of the top (G1-4 and G9-12) and bottom (G5-8 and G13-16) flanges at the middle of the first parallel folds from the middle and vertical support cross-sections. At each location four strain gauges are placed along the flange width in equal distances placed from the flange edges.

Table 2: Orientation and location of measurement devices

Notation	Device	Orientation	Location
T1, T2	linear variable displacement transducers	diagonal	bottom flange at midspan
T3, T4			top flange at midspan
T5	strain gauges	vertical	bottom flange at midspan
T6, T7			support motion
G1-4	strain gauges	longitudinal	upper surface of top flange at midspan
G5-8			upper surface of bottom flange at midspan
G9-12			upper surface of top flange at support
G13-16			upper surface of bottom flange at support

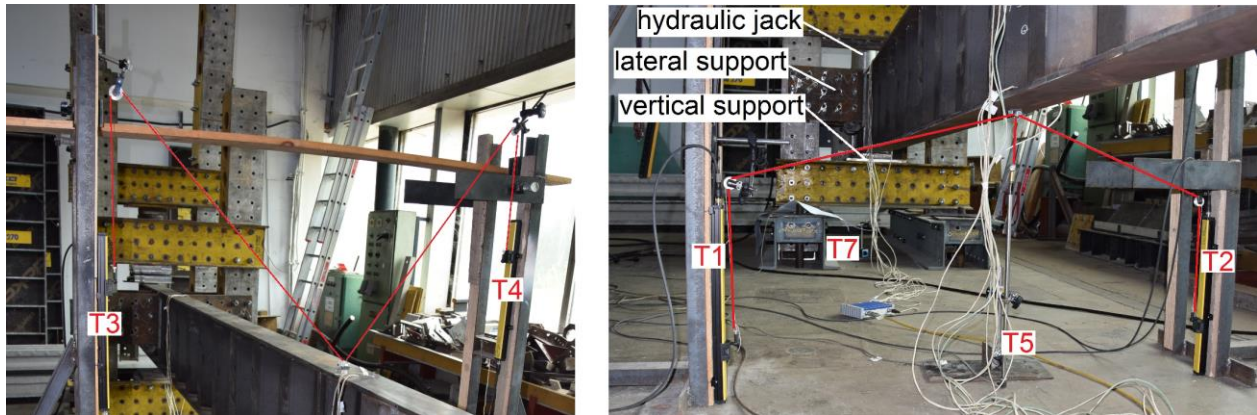


Figure 6: Measurement system of the mid-span cross-section

3.3 Testing procedure

Before testing, the spatial coordinates of the rigid frame measurement system are determined by geodetic triangulation calculations using a total station theodolite from three points to reach high accuracy. Each specimen is loaded under static load. During the loading process up- and unloading loops are executed five times until reaching around 60% of the predicted ultimate load carrying capacity to determine the elastic response of the structure and to determine the stiffness of the analyzed girders in the elastic domain. The measured load-displacement curves of the test specimens are measured during testing and the buckling shapes and the ultimate failure modes are documented on photos to evaluate the results and to compare them by FE simulations. During the tests displacement control is applied and the post-buckling ranges are also studied. After performing the tests steel plate pieces are cut out from the undamaged flange and web parts of each specimen for material testing. The actual material properties (yield and tensile strengths) of all test specimens are determined by standardized tensile coupon test according to ISO 6892-1.

4. Test results

4.1 Overall results and failure modes

The observed ultimate loads and failure modes are presented in Table 3. The cross-section classes of the flanges are 2, 3 and barely 4 according to EN1993-1-1 which validity is proved for trapezoidally corrugated web girders by Jáger et al. (2017a, 2017b). The cross-sectional bending moment resistances are calculated by neglecting the web contribution and by considering only the Steiner's terms as a simplification according to Eqs. 9-12 (EN1993-1-5) for double symmetric sections; where ρ is the reduction factor accounting for local flange buckling based on the effective width method for class 4 flanges proposed by Jáger et al. (2017b). In Eq. 10 c_f is the large flange outstand, η considers the flange-to-web thickness ratio presented by Eq. 11 and R is the enclosing effect of the web corrugation presented by Eq. 12. It is to be noted that the reduction due to local flange buckling is only 2% and 1.5% for specimens 6/1 and 6/2, respectively.

$$M_y = b_f \cdot (\rho \cdot t_f) \cdot f_{yf} (h_w + t_f) \quad (9)$$

$$\rho = \left(14 \cdot \sqrt{\frac{f_{yf}}{235}} \cdot \frac{t_f}{c_f} \right)^\beta \leq 1.0 \quad \text{where } \beta = 5 \cdot \eta \cdot R \cdot \left(\frac{a_4}{a_3} \right)^\eta \quad \text{and } 0.5 \leq \beta \leq 1.0 \quad (10)$$

$$\eta = 0.45 + 0.06 \cdot \frac{t_f}{t_w} \quad (11)$$

$$R = \frac{(a_1 + a_4) \cdot a_3}{(a_1 + 2 \cdot a_4) \cdot b_f} \quad (12)$$



Figure 7: Lateral-torsional buckling failure (LTB) of specimen 1/1

The comparison of the measured LTB resistances and the calculated cross-sectional bending moment resistances are given in Table 3. The failure mode for all specimens is rigid cross-sectional movement and no distortional type failure of the web appeared during the tests. For specimen types #1, #2, #3 and #4 pure lateral-torsional buckling failure (LTB) occurred, while in the case of specimen type #5 the lateral-torsional buckling is followed by local flange buckling

(LTB→LFB) in the post-buckling range. In the case of specimen type #6 the lateral-torsional buckling and local flange buckling are coupled at ultimate load level (LFB+LTB). A typical lateral-torsional buckling failure mode is presented in Fig. 7.

Table 3: Ultimate strengths obtained in the tests

Specimen	c_f/t_f	flange class	M_{test} (kNm)	M_y (kNm)	M_{test}/M_y	failure modes ¹
1/1	7.5	2	297.4	366.2	0.81	LTB
1/2	7.4	2	321.8	374.7	0.86	LTB
2/1	8.1	2	366.0	421.2	0.87	LTB
2/2	8.2	3	351.9	421.4	0.84	LTB
3/1	8.9	3	449.2	481.4	0.93	LTB
3/1	8.8	3	419.9	478.4	0.88	LTB
4/1	8.6	3	720.0	743.8	0.97	LTB
5/1	9.7	3	795.3	837.7	0.95	LTB → LFB
5/2	9.6	3	844.5	841.5	1.00	LTB → LFB
6/1	11.6	4	972.7	932.4	1.04	LFB + LTB
6/2	11.5	4	977.0	945.4	1.03	LFB + LTB

1. LTB = lateral-torsional buckling, LFB = local flange buckling

4.2 Structural behavior

Figures 8-10 show the measured load-displacement curves of each specimen. Curves with the same color represent similar specimens (duplicated tests). In Fig. 8 the relation of the applied bending moment and measured vertical displacement in the middle cross-section is shown. It is to be noted that the initial stiffness increases by using heavier flanges. It can be also observed that proportionally greater displacements are recovered after unloading in case of specimens with larger slenderness to lateral-torsional buckling. This phenomenon could be attributed to the rather elastic buckling of more slender specimens and rather inelastic buckling of specimens having heavier flanges.

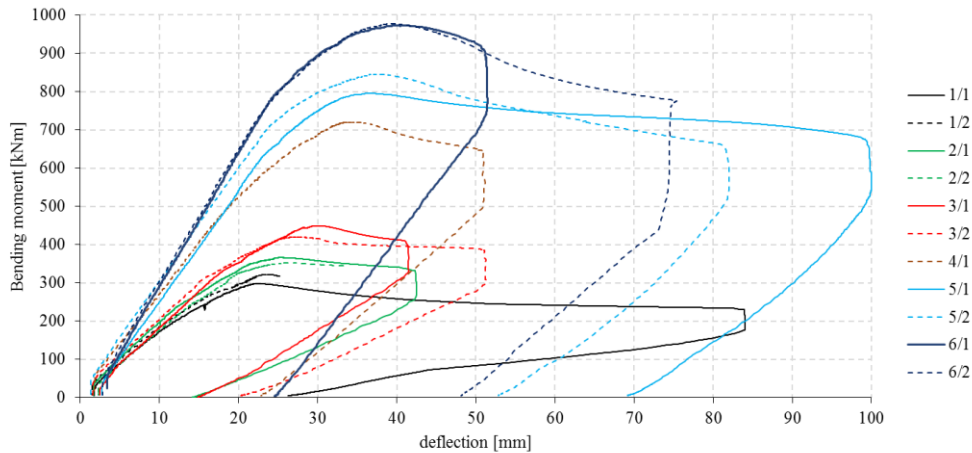


Figure 8: Moment – deflection diagrams of the middle cross-sections

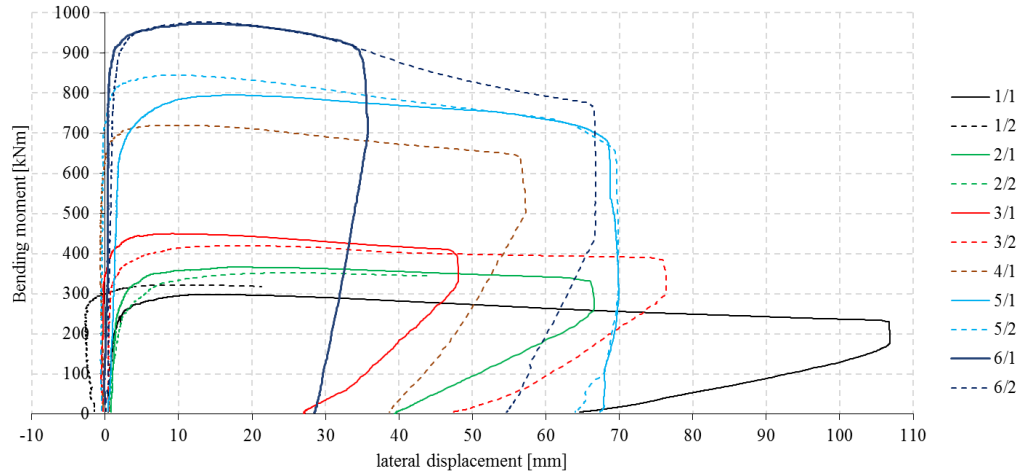


Figure 9: Moment – lateral displacement diagrams of the middle cross-sections

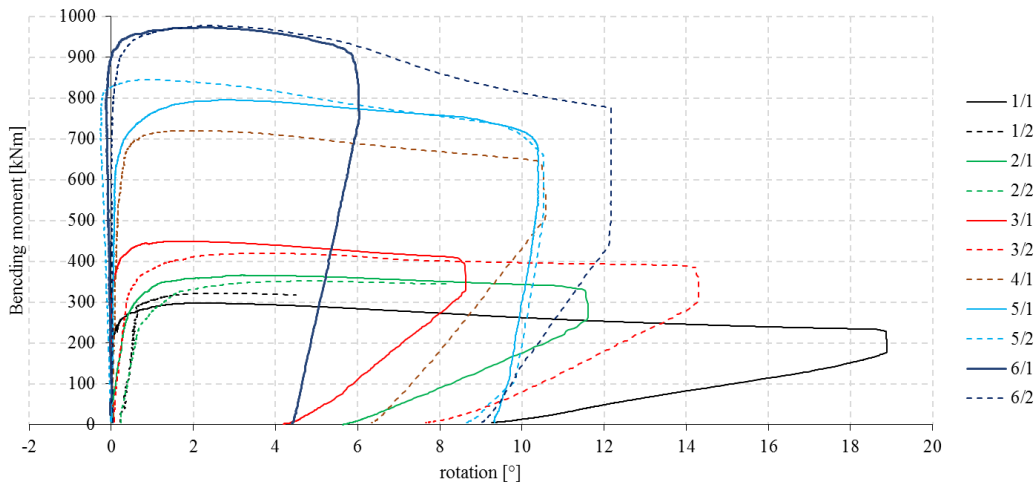


Figure 10: Moment – rotation diagrams of the middle cross-sections

In Figs. 9 and 10 the lateral displacement curves and rotation curves of the middle cross-sections in relation with the applied bending moment are presented. It is to be noted that the lateral displacement and rotation of the middle cross-sections are not necessarily developed simultaneously to the same extent. It is shown that in the case of some slender specimens (1/2, 2/1, 2/2, 3/2) the rotation can develop earlier to a greater extent which is followed by the development of additional lateral displacements before reaching the ultimate load. Furthermore, the test results prove that the magnitude and even the direction of the initial imperfection have significant effect on the ultimate load in the case of slender girders. This can be clearly seen in the case of specimens 1/1 and 1/2, where the imperfection directions are different, resulting in more than 8% resistance increase. Moreover, it can be seen that in case of all specimens the rotations are proportionally recovered in a greater extent than the lateral displacements after unloading. This confirms the previous observation that the rotation is largely allocated in elastic strains. This observation needs further investigation in the future by nonlinear FE analysis on the perfect and imperfect model using different imperfection shapes and magnitudes in order to analyze the effect of imperfections and boundary conditions on the LTB resistance.

5. Comparison with design proposals

Figure 11 presents the comparison of the reduction factors calculated from the test results ($\chi_{LT,test}$) to different lateral-torsional buckling curves of the EN 1993-1-1 ($\beta=0.75$). By the calculation of the relative slenderness three different proposals for the elastic critical moment are used: (i) without any modification in the torsional or warping constants, (ii) with an additional term in the torsional constant proposed by Larsson and Persson (2013) using the correction factor of Lindner (1990) presented by Eq. 5 and (iii) with the slightly modified correction factor of Lindner according to Lopes et al. (2017). In all cases the web contribution to the moment of inertias about the strong and weak axes are ignored. Since the test specimens are restrained against warping and rotation about the weak axis, both effective length factors (k_w and k) are set to 0.5, to maximize the elastic critical moment and provide safe side solution. It is to be noted that all test results are above buckling curve b and the proposal of Lopes et al. (2017) gives the greatest elastic critical moment and the smallest relative slenderness. Table 4 presents the statistical evaluation of the results by taking the ratio of the test and calculated lateral-torsional buckling resistances. The calculated resistances are determined according to Eq. 13 where the reduction factors (χ_{LT}) are obtained from Eqs. 6-8 using the abovementioned three different proposals for the elastic critical moment. It can be seen that the best fit and safe side solution is provided by the proposal of Lopes et al. (2017) using buckling curve b . However, it should be noted that to determine the applicable buckling curve which fits to the safety requirement of the Eurocode, a more complex statistical evaluation should be performed according to EN 1990 Annex D extended by additional FE analysis.

$$M_{b,R} = \chi_{LT} \cdot M_y \quad (13)$$

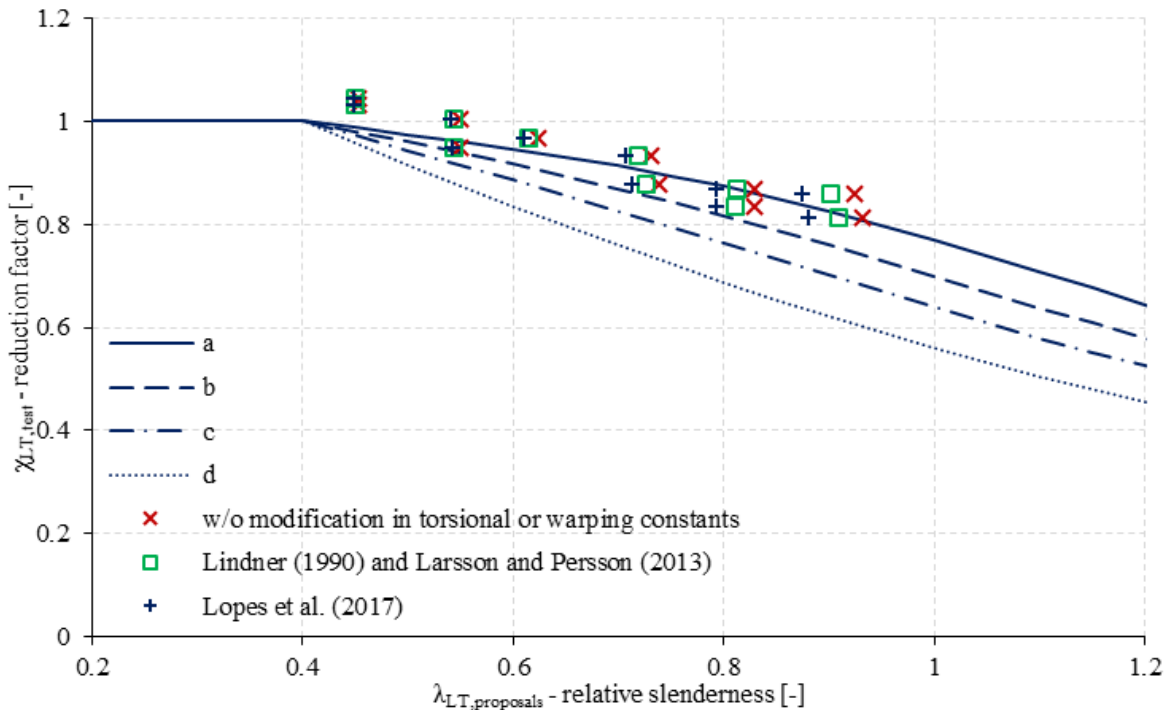


Figure 11: Comparison of the test results and previous proposals with EN1993-1-1 buckling curves

Table 4: Statistical evaluation of the test results and proposals using the EN1993-1-1 buckling curves

	$M_{\text{test}}/M_{b,R,w/o \text{ mod}}$				$M_{\text{test}}/M_{b,R,Lindner}$				$M_{\text{test}}/M_{b,R,Lopes \text{ et al.}}$			
	<i>a</i>	<i>b</i>	<i>c</i>	<i>d</i>	<i>a</i>	<i>b</i>	<i>c</i>	<i>d</i>	<i>a</i>	<i>b</i>	<i>c</i>	<i>d</i>
Average	1.020	1.070	1.124	1.216	1.014	1.061	1.113	1.201	1.008	1.053	1.102	1.186
Std. Dev.	0.030	0.036	0.060	0.107	0.031	0.032	0.052	0.097	0.034	0.028	0.044	0.084
CoV	0.030	0.033	0.053	0.088	0.031	0.030	0.047	0.081	0.034	0.027	0.040	0.071
Min	0.970	1.011	1.038	1.083	0.962	1.008	1.034	1.079	0.952	1.007	1.032	1.076
Max	1.057	1.152	1.253	1.419	1.056	1.131	1.227	1.385	1.056	1.108	1.197	1.346


6. Conclusions

An experimental research program on the lateral-torsional buckling strength of trapezoidally corrugated web girders is presented. Based on the experimental study the following conclusions are drawn:

- for test specimens having compact flanges pure lateral-torsional buckling failure occurred, while in the case of specimens having slender flanges the flange buckling failure coupled with lateral-torsional buckling failure;
- the observed failure mode is rigid cross-sectional movement, no distortional type failure of the web appeared;
- proportionally larger displacements are recovered after unloading for slender specimens attributing to rather elastic buckling and rather inelastic buckling of specimens with heavier flanges;
- the initial imperfections have significant resistance reduction effect on the lateral-torsional buckling strength;
- the test results showed that the lateral-torsional buckling curve *b* of EN1993-1-1 (with $\beta=0.75$ and $\bar{\lambda}_{LT,0}=0.4$) gives lower bound estimate for the prediction of the lateral-torsional buckling strength of trapezoidally corrugated web girders;
- the proposal of Lopes et al. (2017) for the determination of the elastic critical moment provides the best solution together with the lateral-torsional buckling curve *b* of EN1993-1-1 based on the current test results.

Further investigation should be made on the imperfection sensitivity analysis of the test specimens to determine the required imperfection magnitude and direction to be used in the FE analysis and in an extended parametric FE study. Additional numerical simulation results and a more complex statistical evaluation should be also performed to determine the reliable buckling curve for the prediction of the lateral-torsional buckling strength of trapezoidally corrugated web girders which fits to the requirement of the EN 1990.

Acknowledgments

The presented research program is part of the “*BridgeBeam*” R&D project No. GINOP-2.1.1-15-2015-00659; the financial support is gratefully acknowledged. Through the first and second authors the paper was also supported by the  *ÚNKP-18-3-III.* and *ÚNKP-18-4 New National Excellence Program of the Ministry of Human Capacities* and by the *János Bolyai Research Scholarship of the Hungarian Academy of Sciences*; the financial supports are gratefully acknowledged.

References

- Elkawas, A.A., Hassanein, M.F., Elchalakani, M. (2018). "Lateral-torsional buckling strength and behaviour of high-strength steel corrugated web girders for bridge construction." *Thin-Walled Structures*, 122 112-123.
- EN 1990:2005, Eurocode - Bases of structural design.
- EN 1993-1-1:2005, Eurocode 3: Design of steel structures Part 1-1: General rules and rules for buildings.
- EN 1993-1-5:2005, Eurocode 3: Design of steel structures Part 1-5: Plated structural elements.
- Guo, C., Papangelis, J. (2018). "Torsion of beams with corrugated webs." *Proceedings of the Ninth International Conference on Advances in Steel Structures*, Hong Kong, China, 5-7 December, 373-382.
- Hannebauer, D. (2008). "Zur Querschnitts- und Stabtragfähigkeit von Trägern mit profilierten Stegen." *PhD dissertation*, Brandenburgischen Technischen Universität, Cottbus, Germany.
- Ibrahim, S.A. (2014). "Lateral torsional buckling strength of unsymmetrical plate girders with corrugated webs." *Engineering Structures*, 81 123-134.
- Ilanovsky, V. (2015). "Assessment of bending moment resistance of girders with corrugated web." *Pollack Periodica*, 10 (2) 35-44.
- ISO 6892-1:2016, Metallic materials -Tensile testing - Part 1: Method of test at room temperature.
- Jäger, B., Dunai, L., Kövesdi, B. (2016). "Experimental based numerical modelling of girders with trapezoidally corrugated web subjected to combined loading." *Proceedings of the 7th International Conference on Coupled Instabilities in Metal Structures*, Baltimore, Maryland, November 7-8.
- Jäger, B., Dunai, L., Kövesdi, B. (2017a). "Flange buckling behavior of girders with corrugated web Part I: Experimental study." *Thin-Walled Structures*, 118 181-195.
- Jäger, B., Dunai, L., Kövesdi, B. (2017b). "Flange buckling behavior of girders with corrugated web Part II: Numerical study and design method development." *Thin-Walled Structures*, 118 238-252.
- Kazemi, N.K.H.R. (2010). "Lateral bracing of I-girder with corrugated webs under uniform bending." *Journal of Constructional Steel Research*, 66 1502-1509.
- Kubo, M., Watanabe, K. (2007). "Lateral-torsional buckling capacity of steel girders with corrugated web plates." *Doboku Gakkai Ronbunshuu A*, 63 (1) 179-193.
- Larsson, M., Persson, J. (2013). "Lateral-torsional buckling of steel girders with trapezoidally corrugated webs." *MSc thesis*, Gothenburg, Sweden, 57.
- Lindner, J. (1990). "Lateral torsional buckling of beams with trapezoidally corrugated webs." *Proceedings of the 4th International Colloquium on Stability of Steel Structures*, Budapest, Hungary, 79-82.
- Lopes, G.C., Couto, C., Real, P.V., Lopes, N. (2017). "Elastic critical moment of beams with sinusoidally corrugated webs." *Journal of Constructional Steel Research*, 129 185-194.
- Moon, J., Yi, J., Choi, B.H., Lee, H.E. (2009). "Lateral-torsional buckling of I-girder with corrugated webs under uniform bending." *Thin-Walled Structures*, 47 21-30.
- Moon, J., Lim, N.H., Lee, H.E. (2013). "Moment gradient correction factor and inelastic flexural-torsional buckling of I-girders with corrugated steel webs." *Thin-Walled Structures*, 62 18-27.
- Nguyen, N.D., Kim, S.N., Han, S.R., Kang, Y.J. (2010). "Elastic lateral-torsional buckling strength of I girder with trapezoidal web corrugations using a new warping constant under uniform moment." *Engineering Structures*, 32 2157-2165.
- Nguyen, N.D., Han, S.R., Lee, G.S., Kang, Y.J. (2011a). "Moment modification factor of I-girder with trapezoidal-web-corrugations considering concentrated load height effects." *Journal of Constructional Steel Research*, 67 1773-1787.
- Nguyen, N.D., Han, S.R., Kang, Y.J. (2011b). "Lateral-torsional buckling of tapered I-girder with corrugated webs." *The 6th International Symposium on Steel Structures*, Seoul, Korea, November 3-5, 627-634.
- Nguyen, N.D., Han, S.R., Kim, J.H., Kim, S.N., Kang, Y.J. (2012). "Moment modification factors of I-girders with trapezoidal web corrugations under moment gradient." *Thin-Walled Structures*, 57 1-12.
- Pimenta, R.J., Queiroz, G., Diniz, S.M.C. (2015). "Reliability-based design recommendations for sinusoidal-web beams subjected to lateral-torsional buckling." *Engineering Structures*, 84 195-206.
- Sayed-Ahmed, E.Y. (2005). "Lateral torsion-flexure buckling of corrugated web steel girders." *Proceedings of the Institution of Civil Engineers, Structures and Buildings*, 158 (1) 53-69.
- Timoshenko, S.P., Gere, J.M. (1961). "Theory of Elastic Stability.", 2nd edition, *McGraw-Hill*, London.
- Zhang, Z., Li, G., Sun, F. (2011). "Flexural-torsional buckling of H-beams with corrugated webs." *Advanced Materials Research*, 163-167 351-357.
- Zhang, Z., Pei, S., Qu, B. (2017). "Cantilever welded wide-flange beams with sinusoidal corrugations in webs: Full-scale test and design implications." *Engineering Structures*, 144 163-173.